Synthesis, Aromaticity and Application of peri-PentacenoPentacene: Localized Representation of Benzenoid Aromatic Compounds

Tanguy Jousselin-oba, Masashi Mamada, Karen Wright, Jérome Marrot, Chihaya Adachi, Abderrahim Yassar, Michel Frigoli

RESEARCH ARTICLE

Synthesis, Aromaticity and Application of *peri*-PentacenoPentacene: Localized Representation of Benzenoid Aromatic Compounds

Tanguy Jousselin-Oba,[a] Masashi Mamada,*[b] Karen, Wright,[a] Jérome Marrot,[a] Chihaya Adachi,[b,c] Abderrahim Yassar[d] and Michel Frigoli*[a]

In memory of Prof. François Couty

[a] Dr. T. Jousselin-Oba, Dr. K. Wright, Dr. J. Marrot, Dr. M. Frigoli
Institut Lavoisier de Versailles, UMR CNRS 8180
University Paris-Saclay
45 avenue des Etats-Unis, 78035 Versailles Cedex
E-mail: michel.frigoli@uvsq.fr
[b] Dr. M. Mamada, Prof. C. Adachi
Center for Organic Photonics and Electronics Research (OPERA)
Kyushu University
Nishi, Fukuoka 819-0395, Japan
E-mail: mamada@opera.kyushu-u.ac.jp
[c] Prof. C. Adachi
International Institute for Carbon Neutral Energy Research (WPI-I2CNER)
Kyushu University
Nishi, Fukuoka 819-0395, Japan
[d] Dr. A. Yassar
LPICM, UMR CNRS 7647
Ecole Polytechnique
91128 Palaiseau Cedex, France

Supporting information for this article is given via a link at the end of the document.

Abstract: We report the synthesis and optoelectronic properties of TIPS-*peri*-pentacenopentacene (**TIPS-PPP**), a vertical extension of TIPS-pentacene (**TIPS-PEN**), a low band gap material with remarkable stability. We found the synthetic conditions to avoid the competition between 1,2- and 1,4-addition of lithium-acetylide on large aromatic dione. The high stability of **TIPS-PPP** is due to the *peri*-fusion which increases the aromaticity by generating two localized aromatic sextets that are flanked with 2 diene fragments similar to two fused-anthracenes. Like **TIPS-PEN**, **TIPS-PPP** shows the archetypal 2D-brickwall motif in the crystals with a larger transfer integral and smaller reorganization energy. The high mobility of up to 1 $cm^2 V^{-1} s^{-1}$ was obtained in OFET fabricated by wet process. Also, **TIPS-PPP** was used as a near-infrared emitter for NIR-OLED devices resulting in high external quantum efficiency at 800 nm.

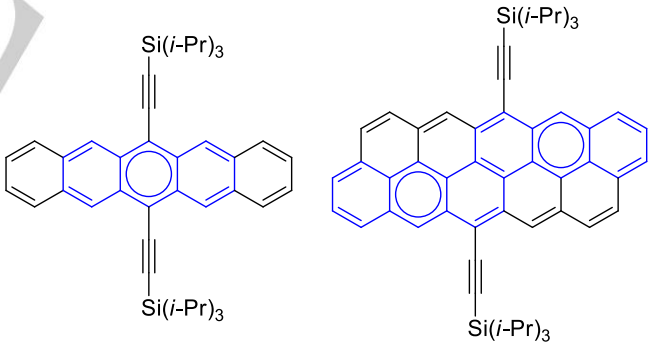

TIPS-PEN
Anthony (2001)

TIPS-PPP
This work

Figure 1. Localized representation (LR) of **TIPS-PEN** and its vertical extension **TIPS-PPP**.

Introduction

In the last two decades, *linear*-acenes composed of laterally fused benzenoid rings have been the subject of intensive study due to fundamental and application significance.[1] They have been used in widespread optoelectronic applications such as organic light-emitting diodes (OLEDs), organic photovoltaic devices to organic field-effect transistors (OFETs).[2-4] Pentacene that shows herringbone edge to face arrangement in the crystals has been the first organic semiconductor to reach hole mobility comparable to that of amorphous silicon.[5-6] Nevertheless, pentacene is extremely reactive and difficult to purify due to its easy oxidation and dimerization.[7] In 2001, Anthony et *al* demonstrated that introducing two triisopropylsilylethynyl groups (TIPS) at the central ring of pentacene core (**TIPS-PEN**), not only increase the solubility and stability by electronic and steric effects and leads to a 2D face to face π-π arrangement and excellent semiconducting characteristics (Figure 1).[8-9]

In addition, as the mobility depends on the crystal packing and the charge reorganization energy that, in turns, depends on the number of π-electrons of the molecules and the conjugation mode,[10-11] longer acenes up to nine rings have been prepared by wet synthesis.[1c], [12] Unfortunately, even **TIPS-Hexacene** degrades promptly in solution via dimerization.[13] Earlier theoretical calculations would suggest that from hexacene onward, these molecules would be a singlet open shell in the ground state but it is still under debate.[14-15] Recently, the lateral benzenoid extension of *peri*-fused systems like pyrene, perylene and anthanthrene has provided low band gap materials with excellent semiconducting characteristics in OFETs with enhanced stability.[16-19] The high stability was ascribed to the enhancement of the global aromaticity thanks to the *peri*-fusion that allows drawing the molecules with two aromatic sextets leading to high distortion energy in interactions with oxygen.[20] An extended Clar's representation for acenoacenes was also proposed.[19] Nevertheless, if the Clar's theory gives uncontested pictures of polyfused systems that are drawn with at least two aromatic sextets (phenanthrene, pyrene, triphenylene, etc..), the Clar's representation of acenes is questionable.[21] According to Clar's theory, acenes are drawn with only one aromatic sextet that migrates over all the rings supposing that all Clar resonance structures have the same weight (Figure 2). This theory is in contrast with some aromatic descriptors suggesting that the middle ring has the highest local aromaticity.[22-23] Along this line, based on molecular electrostatic potential (MESP) analysis or the ring bond order index (RBO), the authors found that the middle ring in acenes is the most aromatic ring and consequently they logically have positioned the aromatic sextet at the center which nevertheless can migrate to the adjacent rings which is here called Weighted representation (Figure 2).[24-26] This raises the fundamental question: which is the proper representation of acenes (Figure 2) ?

In a quest of finding a milestone material for OFET and near infrared (NIR) OLED applications that would combine high stability with low reorganization energy and exhibit the 2D-brickwall motif in the solid state for high OFET mobility and strong emission for OLED, our attention turned to the *peri*-pentacenopentacene (**PPP**) system which can be seen as the vertical extension of the pentacene core (Figure 2). Compared to pentacene ($C_{22}H_{14}$, $C_{4n+2}H_{2n+4}$) that has a D_{2h} symmetry and contains 22 π-electrons, **PPP** ($C_{34}H_{16}$, $C_{4n+4-n}H_{n+6}$) has a C_{2h} symmetry and it is constituted of two rows of pentacene *peri*-fused, so it has 10 benzenoid rings but it contains "only" 34 π-electrons due to the *peri*-fusion, leading that all the rings of one row share π-electrons with the rings of the other row. Introducing the TIPS groups at the center of **PPP** core (**TIPS-PPP**) allows having a ratio between the size of the TIPS groups with the length of the main-axis of the molecule similar to **TIPS-PEN** that could lead to the brickwall motif in the solid state and could be critical of use in OFETs (Figure 1).[8]

Moreover, since **TIPS-anthanthrene**, a smaller homologue of **TIPS-PPP**, absorbs light at 490 nm, slightly lower than **TIPS-tetracene** (540 nm), **TIPS-PPP** would have an absorption maximum close to **TIPS-hexacene** (740 nm) and emits light above 700 nm.[13], [27] Despite recent efforts and progress of NIR-OLED including the development of new organic emitters toward attractive applications,[28] efficient materials for NIR OLED are still rare, so **TIPS-PPP** could be valuable to prepare efficient NIR-OLED devices.

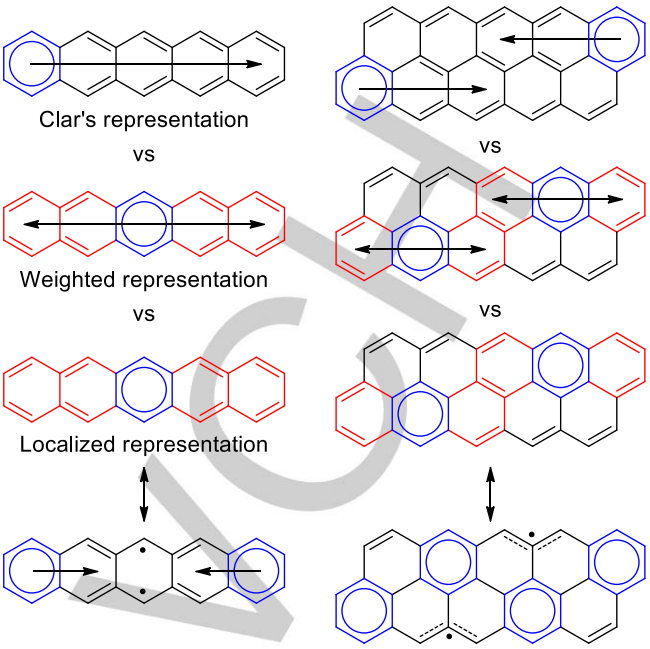

Figure 2. Representation of pentacene and *peri*-pentacenopentacene.

From the viewpoint of synthesis, the preparation of **TIPS-PPP** was challenging because the common method to introduce TIPS group at the right positions is the 1,2-additions of the lithium-acetylide to the corresponding quinone.[29] As observed for large aromatic diones, a competition between 1,2- and 1,4-additions can occur leading to several products being separated with the target molecule at best.[18], [30]

Herein, we disclose the synthetic conditions developed for the synthesis of **TIPS-PPP** from a large aromatic dione and its optoelectronic properties, stability, crystal packing, OFET and OLED performances. In contrast to the Clar's theory, we highlight that in benzenoid systems, the aromatic sextet is localized based on literature data, Nucleus-Independent Chemical Shift (NICS) calculations and the shape of the HOMO molecular orbitals.

Results and Discussion

PPP core has been recently disclosed by Wu's group.[31] The synthetic path does not pass through a dione precursor and does not allow to install proper substituents at the right positions to promote a useful molecular packing in the crystals.

The synthesis of **TIPS-PPP** is depicted in Scheme 1. It is obtained in eight steps starting from 1-methoxypyrene. The first step starts with an *ortho*-lithiation followed by condensation on CO_2 and then methylation of the carboxylate with methyl iodide to provide compound **2** in 64% yield.[32] Then, the methoxy function is turned out into a bromo atom in four steps starting by demethylation (**3**), followed by a triflation (**4**), borylation (**5**) via a cross-coupling reaction and then the conversion of pinacolboronate into a bromo atom using $CuBr_2$ to provide compound **6**.[33] The global yield for this sequence is 65%. Then, **6** is dimerized under Ullmann condition to give compound

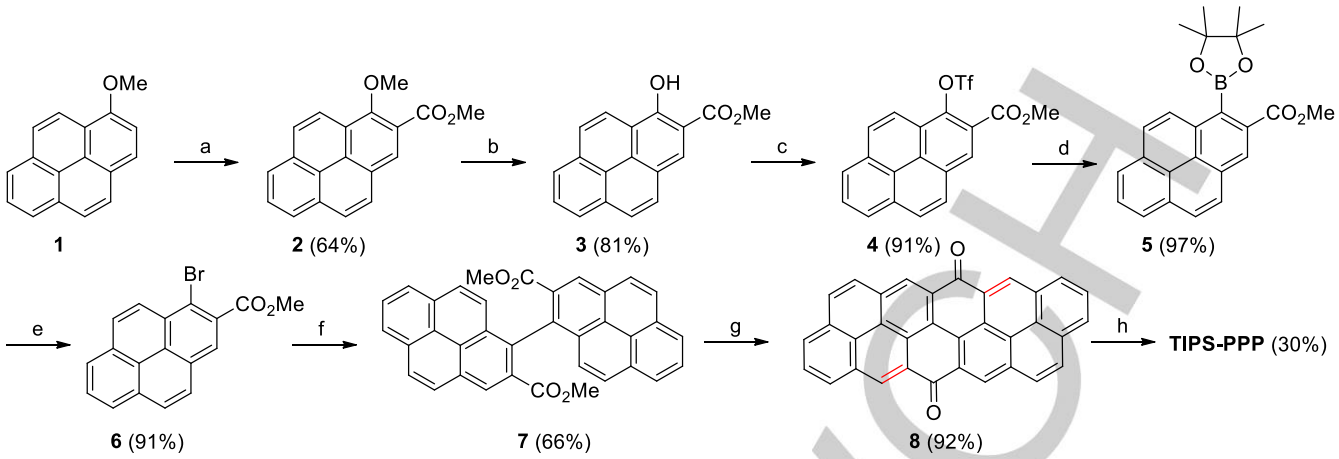

Scheme 1. Synthesis of **TIPS-PPP**. (a) 1) *n*-BuLi, TMEDA, THF, rt, 2) CO_2, rt, 3) MeI, $KHCO_3$, DMF, 45 °C; (b) 1) BBr_3, DCM, −78 °C to −55° C; MeOH, −78 °C; (c) Tf_2O, pyridine, DCM, 0 °C to r.t.; (d) HBPin, $PdCl_2dppf$, NEt_3, toluene, 100 °C; (e) $CuBr_2$, $MeOH/H_2O$, 80 °C; (f) Cu, DMF, 170 °C; (g) TfOH, DCE, 90 °C; (h) 1) TIPSCC-Li, $LaCl_3{\cdot}2LiCl$, THF, 0 °C; 2) $SnCl_2$, toluene, rt.

7 in 66% yield.[34] Then, **7** undergoes double intramolecular Friedel-Crafts acylations using triflic acid as activator to give the large aromatic dione **8** in 92% yield.[35] The introduction of the TIPS groups under the standard condition using 6 equivalents (eq) of the lithium TIPS-acetylide didn't go to completion which is likely due to the insolubility of the dione **8**. Therefore, 20 eq were used instead that lead after the aromatic reductive reaction with tin chloride of the diol intermediate to the formation of the trifunctionalized compound with no trace of the target molecule. This result was not surprising since the ketones of the dione are similar to α,β-unsaturated ketones because it's based on the pyrene ring which has localized double bonds (marked in red in Scheme 1). This problem of competition between 1,2- and 1,4-additions has been encountered with other large aromatic diones but has never been solved.[18], [30] To circumvent this competition, the use of $LaCl_3{\cdot}2LiCl$ as an additive to promote the 1,2-addition in small molecules as developed by Knochel does the job.[36] Adding 20 eq of the acetylide into a THF solution containing the dione and 20 eq of $LaCl_3{\cdot}2LiCl$ furnished the compound solely resulting of 1,2-additions in 30% yield. This result is of great importance for synthetizing nanographenes with the suitable functionality at the right positions from dione precursors.

As mentioned earlier, according to Clar's theory, acenes are drawn with only one aromatic sextet that migrates over all the rings supposing that all Clar resonance structures have the same weight (Figure 2). Earlier theoretical calculations based on NICS indicate that the most aromatic ring in acenes is the middle one since its local diatropic ring current (RC) is the highest, but this statement was under debate.[22], [37] Other theoretical calculations have proposed that the sextet aromatic is rather localized at the centre with possible migration to the adjacent rings (Figure 2).[24-26] However, there is no rationalisation why the sextet aromatic could be localized in the middle of the molecule. As depicted in Figure 2 for the case of pentacene (Supporting Information for the other members), the localisation of the sextet aromatic can be justified with the following arguments:

1) Positioning the aromatic sextet in the middle of the pentacene generates two *ortho*-benzoquinodimethanes (BQDM) while for the other rings, it generates longer *ortho*-quinoidal fragments such as a naphtho- or an anthra-quinodimethane moieties. Knowing that the *ortho*-quinoid molecules like benzo[*c*]thiophene and indeno[2,1-*a*]fluorene have much higher stability than that of their longer homologues, namely, the naphtho[2,3-*c*]thiophene and benzo[*c*]indeno[2,1-*a*]fluorene, respectively, therefore, the localized representation (LR) should have the biggest weight among all the resonance structures since it generates *ortho*-fused dienes units of the lowest dimensionality (Figure 2).[38-39] Also, on top of the middle ring, the two neighbouring rings could formally be written with 6 π-electrons in the two corresponding Kekulé structures. Indeed, with this representation, 3 rings out of 5 can be written with 6 π-electrons even though the only proper aromatic sextet like benzene is the central one (rings in blue, Figure 1).

2) The experimental bond lengths of pentacene for the BQDM parts at the zigzag edge are very similar to that of naphtho[2,3-*c*]thiophene, supporting in an irrefutable manner the LR (Figure 3).[6], [38] Even though they have fixed double bonds, the bond length alternation (BLA) at the zigzag edge decreases from the outer to the central rings likely due to conjugation with equalized bond length at the middle for the pentacene. Moreover, the localization of the fixed double bonds and the sextet aromatic can clearly be seen in the HOMO molecular orbitals for which the orbitals are clearly localized on the double bonds that differ from those localized on the aromatic sextet (Figure 3).

3) It makes sense that between the closed- and open-shell resonance forms that the aromatic sextet is not localized on the same ring due to the reorganization of π-electrons (Figure 2).

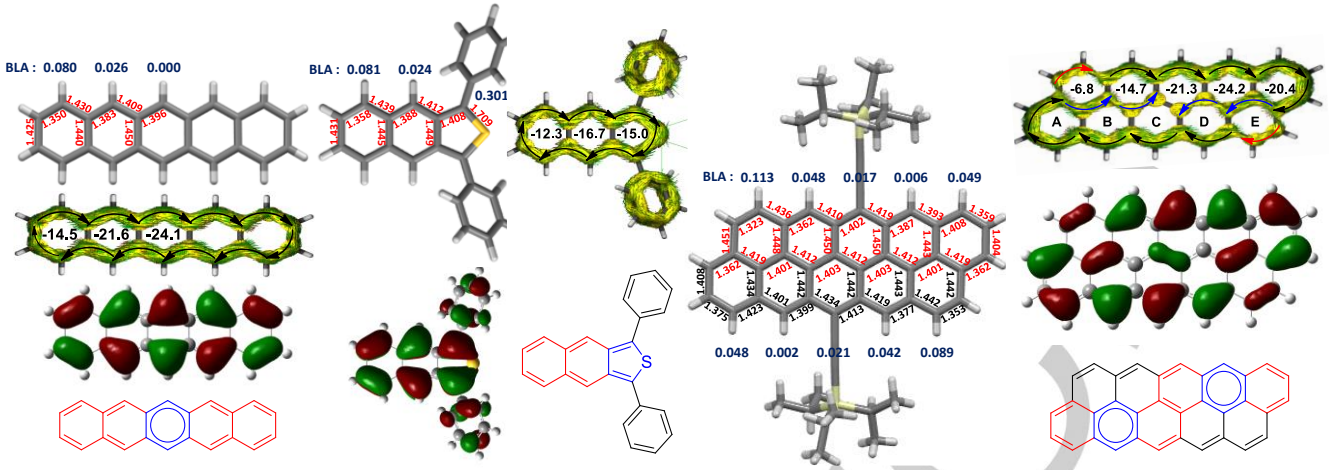

Figure 3. X-ray structures,[6], [36] NICS(1.7)πzz,[39] ACID plots[38] and HOMO of pentacene, naphtho[2,3-*c*]thiophene and **TIPS-PPP**.

4) It is well known that the NICS values increase from the outer to the middle ring in acenes.[22] These results were attributed to the presence of local- and semi-local RCs along with the global one that could have been right with the Clar's representation.[37] Actually, the ACID plot of naphtho[2,3-*c*]thiophene is very informative (Figure 3).[40] Even though this molecule has an *ortho*-quinoid structure with fixed double bonds, the shape of the ACID plot is the same as that of pentacene with the observation of one global RC positioned at the periphery. Since there is no local RC around the thiophene which is the only proper aromatic ring of the molecule, the occurrence of RCs other than the global one in acenes seems to be unlikely. Therefore, the increase of the NICS (1.7)πzz[41] values from the outer- to the central ring is due to a decrease of the BLA at the zigzag edge which is correlated to the electron density. For pentacene, the NICS value is the highest in the middle ring since the latter is an aromatic sextet with equalized bond lengths. Within simple benzenoid molecules, a higher local NICS value of a ring means in principle that this ring holds the sextet aromatic. However, NICS should be interpret with caution. In contrast, the comparison of local NICS values between molecules is not relevant since the NICS values increase with the decrease of the BLA at the zigzag edge and the increase of the number of π-electrons involved in the global RC. For instance, the NICS value of benzene is −16.5 ppm which is lower than that of naphthalene (−18.0 ppm) that has a larger BLA at the zigzag edge and lower aromaticity. In a similar manner, the NICS of the aromatic sextet within the LR of acenes increases from anthracene (−21.7 ppm) to pentacene (−24.1 ppm) (Table S4).

All these above elements indicate that the LR of acenes is the representation that should be stated in the future.

Accordingly, linear-acenes exhibit global aromaticity with 4n+2 π-electrons (Hückel's rule) at the periphery generating a diatropic ring current under magnetic field. They are conjugated molecules containing only one aromatic sextet in the middle flanked with ortho-fused-dienes. From anthracene onward, only 3 rings can formally be written with 6 π-electrons indicating that the global aromaticity of acenes decreases with the size due to an increase of the number of non-aromatic ortho-fused-dienes.

TIPS-PPP has rather low solubility in common organic solvents. Single crystals suitable for X-ray analysis were grown from chlorobenzene solution. The X-ray bond lengths (in red) are depicted in Figure 3 along with those calculated at R-B3LYP level of theory (in black).[42] The X-ray bond lengths are essentially shorter than the ones calculated likely due to the reliability factor (R) being above 0.05 (0.075). However, the BLA of the bonds at the zigzag edge between experimental and calculated ones are nearly the same for all the rings except for ring E that shows the highest BLA. As expected, the BLA decreases from the outer to the central rings even though it is ring B that shows practically equalized bond lengths and so indicates that ring bears the aromatic sextet (Figures 1-2). As a consequence, ring B exhibits the highest local diatropic RC. On the contrary, ring E sustains the lowest diatropic RC since its BLA at the zigzag edge is the largest. Positioning the two aromatic sextets on ring B generates ortho-diene fragments on the rings A and C while rings D and E have only one single double bond. Since rings A and C can formally be written with 6 π-electrons, they should have higher NICS values than rings D and E even though rings A and D have similar BLA. Indeed, after ring B, rings A and C have the second highest NICS values which are similar to each other even though ring C has lower BLA due to its central position leading to a higher conjugation at the zigzag edge. Ring D has a higher NICS value than ring E due to a lower BLA. As can be seen from the ACID plot, the diatropic RC is well observed at the zigzag edge indicating that the molecule is globally aromatic with 26 π-electrons at the periphery (4n+2). There is also a trans-annular RC (arrows in blue) that makes the local NICS values of rings E and D even lower since it corresponds to a paratropic RC for them and explains the discordancy between BLA and NICS values of rings A and D. In a similar manner, ring A supports a fully diatroptic RC around itself but not ring C making NICS values similar for both while having different BLA. The molecular orbital at the zigzag edge of ring B that holds the aromatic sextet differs from the other orbitals. Accordingly, **PPP** can be drawn with two localized aromatic sextets flanked with two diene units similar to two fused-anthracenes. In general, for closed-shell molecules, the ring that has the smallest BLA at the zigzag edge can be safely written as the aromatic sextet of the molecule. In the case of two neighbouring rings having the same BLA like in even acenes

(naphthalene, tetracene, etc), the sextet aromatic is shared by the two rings. For some cases, NICS values may be slightly different depending on the annelation of these two rings like for anthanthrene for instance. The LR of *peri*-acenoacenes and acenoacenes derivatised from anthanthrene are shown in the supporting information (Figures S10–11).

In toluene solution, **TIPS-PPP** displays a blue-green colour with an absorption maximum (λ_{max}) at 726 nm (Figure 4a and Table 1). TD-DFT calculations at ωB97XD/6-311+G(d,p) level predict well this transition (λ_{max} = 734 nm with oscillator strength (*f*) = 0.55), Table S5). It should be noted that introducing TIPS group on the aromatic sextets (rings B) of the **PPP** core instead does not alter the λ_{max} (735 nm, *f* = 0.66) This theoretical result indicates that the radical cation and anion are stabilized in a similar manner on both rings B and C which is consistent with the main resonance form of the diradical (Figure 2). **TIPS-PPP** absorbs at a longer wavelength than **TIPS-PEN** (643 nm) but a slightly lower wavelength than **TIPS-hexacene** (740 nm).[13] As mentioned earlier, **PPP** has 26 π-electrons at the periphery, the same number of π-electrons as **hexacene**.

TIPS-PPP exhibits fluorescence in oxygen-free toluene solution with emission maximum (λ_{em}) at 739 nm and a fluorescence quantum yield (Φ_{em}) of 26.5 % (Figure 4a, Table 1). A very small Stokes shift of 27 cm^{-1} was obtained, contrary to **TIPS-PEN** which emits light at 652 nm with a larger Φ_{em} that reaches a value of 44 % and a Stokes shift of 215 cm^{-1}. The total fluorescence lifetime (τ_f) of **TIPS-PPP** is twice lower than that of **TIPS-PEN** even though the radiative decay rate constants (k_r) for both are very similar. Consequently, the lower Φ_{em} observed for **TIPS-PPP** is due to an increase of the nonradiative deactivation rate constant (k_{nr}) likely owing to the gap law.[43] According to the expression of k_{nr}, k_{nr} increases exponentially with the decrease of the energy gap (Δ*E*), which may be a practically unsolvable problem for the decrease of PLQY with the decrease of Δ*E*.[44] However, k_{nr} can be reduced with a smaller excitation reorganization energy (λ_M).[44] In fact, the calculated λ_M for **TIPS-PPP** is much smaller than that of **TIPS-PEN** (Table S2), suggesting that the two-dimensional rigid molecular design along with an increase of π-electrons is an effective strategy for developing NIR emitters. The emission properties of **TIPS-PPP** were also investigated in different solvents. A positive solvatochromism is observed and emission spectra reach nearly 800 nm in polar solvents while still keeping PLQY in a high value of ca. 10% (Figure S4, Table S1). These results underline the potential of **TIPS-PPP** for the fabrication of NIR-OLED devices. Further discussions of emission properties of **TIPS-PPP** are shown in the OLED section (vide infra).

Cyclic voltammetry (CV) was performed in chlorobenzene and half-wave potentials were determined relative to Fc/Fc^+ (Figure 4b). **TIPS-PPP** exhibits two reversible reduction and oxidation peaks. Half-wave potentials of the first oxidation/reduction peaks were at 0.13/−1.36 V. From these values, the HOMO/LUMO energy levels were found to be −4.93/−3.44 eV which corresponds to an electrochemical energy gap of 1.49 eV.

Stability tests of **TIPS-PPP** and **TIPS-PEN** were performed in air-saturated-toluene solution in a lightening laboratory (Figure 4c). **TIPS-PEN** has a half-life ($\tau_{1/2}$) of 1.4 days whereas **TIPS-PPP** has an improved stability with a $\tau_{1/2}$ of 22 days. This stability 16 times superior can be attributed to the fact that **TIPS-PPP** absorbs less visible light than **TIPS-PEN** and **TIPS-PPP** has higher aromaticity since it is written with two aromatic sextets flanked with two *ortho*-fused-diene units similar to two fused-anthracenes. It should be noted that there is an acceleration of the degradation speed over time (Figure 4c, Figure S1). As seen recently for a tetracenotetracene derivative, this is likely due to the formation of a dione that photosensitizes singlet oxygen.[19a] Indeed, the absorption spectrum after 45 days does not show clear patterns, indicative of the presence of several photoproducts (Figure 4d). Nevertheless, one can distinguish absorption maxima at 417 nm and 580 nm. The latter may be attributed to the formation of the dione resulting in the addition of oxygen on rings B (Figure S2). The former may be ascribed to the absorption of a pyrene like molecule that would result in the attack of oxygen on rings C. These results are in line with Hückel molecular orbital localization energy calculation made on **PPP** that suggests that rings B and C are the most reactive.[45] They are indeed the two richest rings in electrons giving photodegradation products with the highest thermodynamic stabilities.

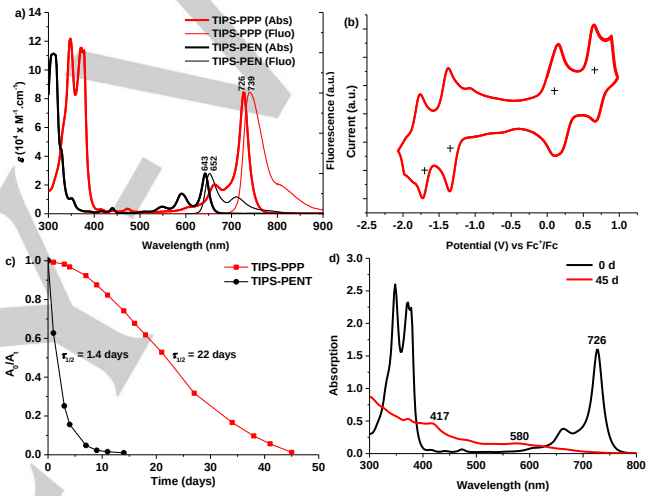

Figure 4. Optical and electrochemical properties of **TIPS-PPP**: (a) UV/vis spectrum in toluene; (b) CV in chlorobenzene with 0.1M $Bu_4N.PF_6$ as the supporting electrode; (c) Change of UV/vis absorption (followed at their own λ_{max}) over time in toluene (25 μM) of **TIPS-PPP** compared to **TIPS-PEN**; (d) Absorption of **TIPS-PPP** before and after 45 days in lightening laboratory.

Table 1. Photophysical properties of **TIPS-PPP** and **TIPS-PEN**.[a]

Compd	λ_{abs} (nm)	λ_{em} (nm)	Φ_{em}[b] (%)	SS[c] (cm^{-1})	τ[d] (ns)	k_r[e] (s^{-1})	k_{nr}[f] (s^{-1})
TIPS-PPP	726	739	26.5	27.0	8.1	3.3×10^7	9.0×10^7
TIPS-PEN	643	652	44.0	215	16.8	2.6×10^7	3.3×10^7

[a] In toluene solution in inert atmosphere. [b] Absolute value. [c] Stokes shift. [d] Fluorescence lifetime. [e] Radiative decay rate constant calculated from $k_r = \Phi_{emi} / \tau$. [f] Nonradiative deactivation rate constant calculated from $\tau = 1/(k_r + k_{nr})$.

Since **TIPS-PPP** is an acene-like molecule absorbing in the same region as **TIPS-hexacene**, the calculation of the diradical character was investigated. It was estimated from the electron occupancies of the frontier natural orbitals through the Yamaguchi's scheme (y_0) at UHF/6-31G(d,p) level of theory.[46] Both have similar diradical characters in a range of 0.58–0.61 and singlet-triplet energy gap ($\Delta E_{S\text{-}T}$) around 8.5 kcal.mol^{-1} (Tables S6–7). These theoritical results indicate that the gain of the aromaticity of the open-shell form compared to the closed-shell one for **hexacene** and **PPP** is similar. For **PPP**, the gain of aromaticity should be understanding as going from two fused-anthracenes in the closed-shell form (2 aromatic sexets) to two fused-pyrenes in the open-shell one (4 aromatic sexets). Even though the calculations at B3LYP level would suggest that they have an open shell ground state, this statement is unlikely since both do not show the weak absorption after the λ_{max} corresponding to the HOMO, HOMO / LUMO, LUMO doubly excited state (DES), typically observed for diradicaloid systems.[47] On top of that, the LR of the closed-shell structure of hexacene indicates the number of formally non- (rings in red) and aromatic rings (rings in blue) is identical (Figure 5). Even though the DES is observed for heptacene derivatives for which the number of non-aromatic rings surpasses one of aromatic rings,[48] the calculated bond lengths at B3LYP level of hexacene and heptacene show a decrease of the BLA going from the outer to the inner rings while the bond lengths of the rings in red are similar to the BDQM part of pentacene (rings in red in Figure 3) which likely support their closed shell nature and LR (Figure S9).[15] In a similar manner, the calculated bond lengths of **PPP** and *peri*-tetracenotetracene (**PTT**) are similar for the outer rings because they are in the same π-conjugated environement as can be seen from their LR (Figure S10).

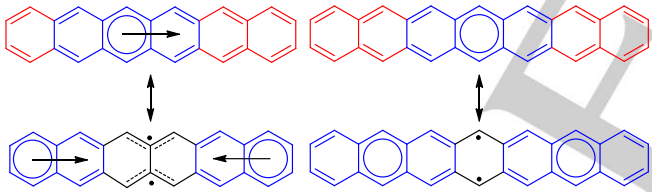

Figure 5. LR of hexacene and heptacene and their main open-shell resonance forms.

Pleasingly, **TIPS-PPP** shows the archetypal 2D-brickwall motif as **TIPS-PEN** in the crystals (Figure 6). Both compounds give crystals with a triclinic symmetry with a *P*-1 space group. For **TIPS-PPP**, each molecule in red is in π–π interactions with four neighbouring molecules. There are six closed contacts between the molecules in red and blue with distances spanning from 3.38 to 3.43 Å and 4 closed contacts between the red and the green molecules with distances around 3.70 Å. Transfer integrals (t_n) between the HOMOs of **TIPS-PPP** and **TIPS-PEN** in their packing structures using DFT calculations at the Gaussian PW91 level of theory were calculated (Figure 6 and Table 2).[10] In contrast to **TIPS-PEN** that shows anisotropic transfer integrals, the transfer integrals for **TIPS-PPP** are fairly well-balanced and are stronger. The reorganization energy for holes (λ_h) was also calculated at B3LYP level that shows, as expected, that **PPP** has a λ_h less important than that of pentacene, ascribed to a number of π-electron more important (Table 2).[10-11] The estimated hole mobility (μ_h) of charge hopping based on the Marcus-Hush theory of **TIPS-PPP** was found to be around one order of magnitude higher than that of **TIPS-PEN** (Table 2).[49] According to these calculations, **TIPS-PPP** has intrinsically a much better semiconducting behaviour than **TIPS-PEN**. Since **TIPS-PPP** shows excellent molecular packing, its OFET performances in thin-film fabricated from a drop casting method, was evaluated. The device configurations were bottom-gate/top-contact (BG/TC) with cross-linked poly-vinylphenol (PVP) on SiO_2/Si substrate and top-gate/bottom-contact (TG/BC) with CYTOP dielectric, as shown in Figure 7. **TIPS-PPP** showed clear hole transport characteristics although the electron transport was very poor showing only a weak gate-effect at high voltage (Figures 7a–7b). The hole mobility of BG/TC devices was 0.33 cm^2 V^{-1} s^{-1} while electron mobility was 4 × 10^{-4} cm^2 V^{-1} s^{-1} with a very high threshold voltage. The TG/BC device showed an improved hole mobility up to 1.0 cm^2 V^{-1} s^{-1} with a threshold voltage of 1 V (Figures 7c–7d). Although this mobility is relatively higher than that of ~0.3 cm^2 V^{-1} s^{-1} for **TIPS-PEN** obtained for devices fabricated in similar conditions,[50] the comparison of theoretical and experimental mobilities indicates that the carrier transport properties of **TIPS-PPP** still have room for improvement, i.e. by increasing the size of single crystalline domain.

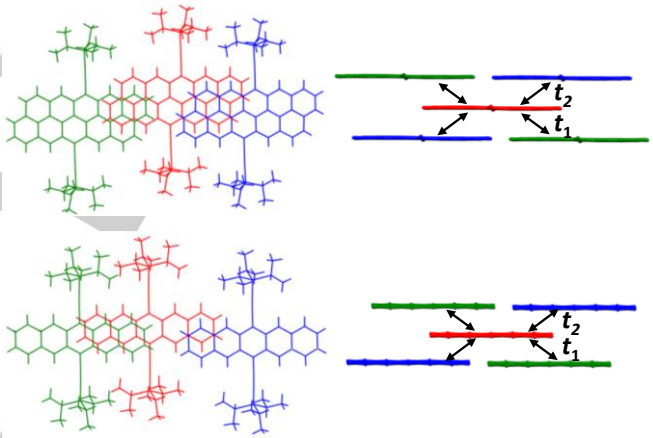

Figure 6. Packing of **TIPS-PPP** and **TIPS-PEN**.

Table 2. Transfer integrals and charge reorganization energy (holes) of **TIPS-PPP** and **TIPS-PEN**.

Compounds[]	t_1 (mev)[a]	t_2 (mev)[a]]	λ_h (meV)[b]	μ_h (cm^2 V^{-1} s^{-1})[c]
TIPS-PPP	43.49	-29.17	85	2.61
TIPS-PEN	-2.78	23.81	119	0.32

[a] Calculated at the Gaussian PW91. [b] Charge reorganization energy calculated at B3LYP/6-311+G(d,p) for **TMS- PPP** and **TMS-PEN**. [c] Calculated drift hole mobility.

The NIR-OLEDs using **TIPS-PPP** were investigated using a thermally activated delayed fluorescence (TADF)-assisted fluorescence (TAF) system to harvest triplet excitons generated upon charge carrier recombination.[51] Since the **TIPS-PPP** absorbs between 600–750 nm, 7,10-bis[4-(diphenylamino)phenyl]-2,3-dicyanopyrazinophenanthrene (**TPA-DCPP**) was selected because its strong red emission overlaps the absorption of **TIPS-PPP**.[52] Thus, photophysical properties for spin-coated thin-films with different doping concentrations in host

material of 4,4'-bis(carbazol-9-yl)biphenyl (CBP) were firstly investigated (Table S3, Figure S7). Interestingly, the emission maxima were red-shifted with the increase of **TPA-DCPP** concentration because of the polar donor-acceptor structure of the TADF material while keeping PLQY in nearly the same value of 13% for 0.5 wt% **TIPS-PPP** films. Thus, the concentration of **TPA-DCPP** was fixed to 50 wt% for TAF-OLEDs. Because of the low doping concentration used of only 0.5 wt% for **TIPS-PPP**, emission from **TPA-DCPP** is not negligible. The increase of **TIPS-PPP** concentration from 0.5 to 1.5 wt% reduces **TPA-DCPP** emission along with further red-shifting of **TIPS-PPP** emission (>800 nm) although PLQY is slightly decreased by concentration quenching.

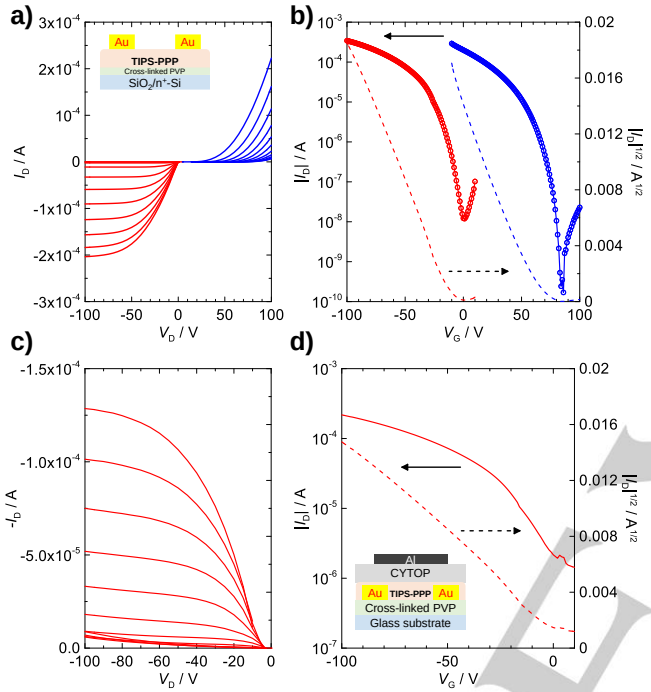

Figure 7. OFET devices of **TIPS-PPP**. a) Output and b) transfer characteristics of a BG/TC device. c) Output and d) transfer characteristics of a TG/BC device.

The device structure of OLEDs was ITO/PEDOT:PSS (30 nm)/emissive layer (EML) (45 nm)/ 2,4,6-tris(biphenyl-3-yl)-1,3,5-triazine (T2T) (10 nm)/2,7-bis(2,20-bipyridine-5-yl)triphenylene (BPy-TP2) (50 nm)/8-quinolinato lithium (Liq) (2 nm)/aluminum (Al) (100 nm). The EML consisting of x wt% **TIPS-PPP** (x = 0.5 for Device A, 1.0 for Device B, and 1.5 for Device C), 50 wt% DPA-DCPP, and 50 – x wt% CBP was spin-coated from chloroform solution, followed by vacuum deposition for upper layers. The electroluminescence (EL) spectra were nearly the same as the PL spectra for the corresponding EML films (Figure 8a and Figure S7), resulting in relatively large emission from TPA-DCPP for Device A. Since the narrow gap materials cause carrier trap, Device C with high doping concentration of 1.5 wt% for **TIPS-PPP** showed lower external quantum efficiency (EQE, η_{ext}) (Figures 8b-c). Therefore, the best EQE was 0.6% at 800 nm obtained for Device B. This performance is considered to be significant since there are a very limited number of OLEDs at >800 nm, which are summarized in recent papers (Figure 8d).[53,54] The ideal EQE was estimated to be 1.8% from PLQY and out-coupling efficiency calculated by optical simulation for this device structure (Figure S8). This difference is attributed to direct carrier recombination in **TIPS-PPP** as observed in many NIR emitters-based OLEDs, indicating a high potential for further improvement of the OLED performances. Overall, a new perspective on acene-like molecules with applications in NIR emitters has been successfully demonstrated.

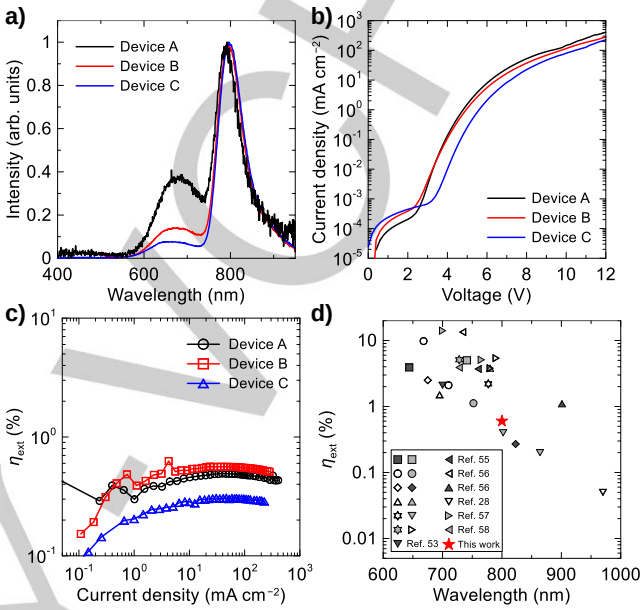

Figure 8. a) EL spectra of **TIPS-PPP** with different doping concentrations (0.5, 1.0, and 1.5 wt%) in TPA-DCPP and CBP. b) Current-density (*J*)-voltage (*V*) characteristics. c) EQE as a function of *J*. d) EQE versus wavelength based on the summary in ref. 53 with some recent papers.

Conclusion

20 years after the first synthesis of the famous **TIPS-PEN**, its vertical extension namely TIPS-*peri*-pentacenopentacene (**TIPS-PPP**) has been prepared. The synthetic conditions to avoid the competition between 1,2- and 1,4-additions of lithium acetylide on large aromatic dione have been disclosed. This constitutes a major advance in the synthesis of nanographenes that would allow to introduce the right substitutions at the right positions from dione precursors. A localized representation of acenes has been highlighted. The latter should be considered as conjugated molecules containing a localized aromatic sextet in the middle flanked with *ortho*-fused-dienes. They exhibit global aromaticity with 4n+2 π-electrons (Hückel's rule) at the periphery generating a diatropic ring current under magnetic field. **TIPS-PPP** and **TIPS-hexacene** have 26 π-electrons at the periphery and absorb at similar wavelengths. Both compounds have similar diradical characters but cannot be classified as diradicaloid with an open-shell ground state. **TIPS-PPP** exhibits a remarkable half-life of 22 days in toluene solution and its stability is 16 times superior than that of **TIPS-PEN**. This high stability is justified by the *peri*-fusion that increases the aromaticity by generating two aromatic sextets which each are flanked with 2 dienes similar to two fused-anthracenes. Like **TIPS-PEN**, **TIPS-PPP** exhibits a 2D-brickwall motif in the solid state with stronger π–π interactions and a smaller reorganization energy. OFET devices were fabricated using a wet deposition process and the hole mobility found is as

high as 1 cm^2 V^{-1} s^{-1}. Nevertheless, single-crystal OFETs with **TIPS-PPP** should provide much higher mobility and this would be disclosed in due course. The NIR-OLED performance at 800 nm of **TIPS-PPP** suggests that acene-like materials can be critical of use for the preparation of efficient NIR-emitters.

Acknowledgements

M.F. and A.Y. acknowledge financial support from the Agence Nationale de la Recherche ANR-16-CE07-0024 (GATE). M.M. acknowledges financial support from JST ERATO Grant Number JPMJER1305, JSPS KAKENHI Grant Number 19H02790 and 21H05401, Inamori Foundation and Iketani Science and Technology Foundation.

Keywords: Aromaticity • Acenoacenes • Structure elucidation • Clar's representation • OLED

[1] a) M. Bendikov, F. Wudl and D. F. Perepichka, *Chem. Rev.* **2004**, *104*, 4891-4946; b) J. E. Anthony, *Angew. Chem. Int. Ed.* **2008**, *47*, 452-483; *Angew. Chem.* **2008**, *120*, 460-492; c) Q. Ye, C. Chi, *Chem. Mater.* **2014**, *26*, 4046-4056.

[2] H. Sirringhaus, *Adv. Mater*. **2014**, *26*, 1319-1335

[3] J. Roncali, P. Leriche, P. Blanchard, *Adv. Mater.* **2014**, 26, 3821-3838.

[4] a) J. Mei, Y. Diao, A. L. Appleton, L. Fang, Z. Bao, *J. Am. Chem. Soc.* **2013**, *135*, 6724-6746; b) G. Schweicher, G. Garbay, R. m. Jouclas, F. o. Vibert, F. l. Devaux, Y. H. Geerts, *Adv. Mater.* **2020**, *32*, 1905909.

[5] L. Yen-Yi, D. I. Gundlach, S. F. Nelson, T. N. Jackson, *IEEE Trans. Electron Devices Lett.* **1997**, *44*, 1325-1331.

[6] Article mentioned for the X-ray structure: T.Siegrist, C. Kloc, J.H. Schon, B. Batlogg, R.C. Haddon, S. Berg, G.A. Thomas, *Angew. Chem. Int. Ed.* **2001**, *40*, 1732-1736; *Angew. Chem.* **2001**, *113*, 1782-1786.

[7] P. T. Herwig, K. Müllen, *Adv. Mater.* **1999**, *11*, 480-483.

[8] J. E. Anthony, J. S. Brooks, D. L. Eaton, S. R. Parkin, *J. Am. Chem. Soc.* **2001**, *123*, 9482-9483.

[9] A. Maliakal, K. Raghavachari, H. Katz, E. Chandross, T. Siegrist, *Chem. Mater.* **2004**, *16*, 4980-4986

[10] W.-Q. Deng, W. A. Goddard, *J. Phys. Chem. B* **2004**, *108*, 8614

[11] J.-L. Brédas, D. Beljonne, V. Coropceanu, J. Cornil, *Chem. Rev.* **2004**,*104*, 4971−5003.

[12] J. E. Anthony, *Isr. J. Chem.* **2014**, *54*, 642-649.

[13] B. Purushothaman, S. R. Parkin, J. E. Anthony, *Org. Lett.* **2010**, *12*, 2060–2063.

[14] M. Bendikov, H. M. Duong, K. Starkey, K. N. Houk, E. A. Carter, F. Wudl, *J. Am. Chem. Soc.* **2004**, *126*, 7416–7417.

[15] Y. Yang, E. R. Davidson, W. Yang, *PNAS,* **2016**, *113*, E5098-E5107.

[16] L. Zhang, A. Fonari, Y. Liu, A.-L. M. Hoyt, H. Lee, D. Granger, S. Parkin, T. P. Russell, J. E. Anthony, J.-L. Brédas, V. Coropceanu, A. L. Briseno, *J. Am. Chem. Soc.* **2014**, *136*, 9248-9251.

[17] X. Liu, M. Chen, C. Xiao, N. Xue, L. Zhang, *Org. Lett.* **2018**, 20, 15, 4512–4515.

[18] Z. Wang, R. Li, Y. Chen, Y.-Z. Tan, Z. Tu, X. J. Gao, H. Dong, Y. Yi, Y. Zhang, W. Hu, K. Müllen, L. Chen, *J. Mater. Chem. C.* **2017**, *5*, 1308-1312.

[19] a) K. Sbargoud, M. Mamada, T. Jousselin-Oba, Y. Takeda, S. Tokito, A. Yassar, J. Marrot, M. Frigoli, *Chem. Eur. J.* **2017**, *23*, 5076 –5080, b) T. Jousselin-Oba, M. Mamada, J. Marrot, A. Maignan, C. Adachi, A. Yassar, M. Frigoli, *J. Am. Chem. Soc.* **2019**, *141*, 9373-9381.

[20] S. Thomas, J. Ly, L. Zhang, A. L. Briseno, J.-L. Brédas, *Chem. Mater.* **2016**, *28*, 8504–8512.

[21] M. Solà, *Front. Chem.* **2013**, *1*, 1-8.

[22] a) P. v. R. Schleyer, M. Manoharan, H. Jiao, F. Stahl, *Org. Lett.* **2001**, *3*, 3643–3646; b) R. Gershoni-Poranne, A. Stanger, *Chem. Soc. Rev.***, 2015**, 44**,** 6597-6615.

[23] a) G. Portella, J. Poater, J. M. Bofill, P. Alemany, M. Solà, *J. Org. Chem.* **2005**, *70*, 2509–2521; b) D. Yu, T. Stuyver, C. Rong, M. Alonso, T. Lu, F. De Proft, P. Geerlings, S. Liu, *Phys. Chem. Chem. Phys*. **2019**, *21*, 18195—18210.

[24] a) C. H. Suresh, S. R. Gadre, *J. Org. Chem.* **1999**, *64*, 2505–2512; b) K. Anjalikrishna, C. H. Suresh, S. R. Gadre, *J. Phys. Chem. A*, **2019**, *123*, 10139–1015.

[25] M. Randić, A. T. Balaban, *Int. J. Quantum Chem*. **2018**, *118*, E25657.

[26] D. W. Szczepanik, M. Solà, T. M. Krygowski, H. Szatylowicz, M. Andrzejak, B. Pawelek, J. Dominikowska, M. Kukulka, K. Dyduch, *Phys. Chem. Chem. Phys.* **2018**, *20*, 13430-13436.

[27] L. Zhang, B. Walker, F. Liu, N. S. Colella, S. C. B. Mannsfeld, J. J. Watkins, T.-Q. Nguyen, A. L. Briseno, *J. Mater. Chem.* **2012**, *22*, 4266-4268.

[28] A. Zampetti, A. Minotto, F. Cacialli, *Adv. Funct. Mater.* **2019**, *29*, 1807623.

[29] J. L. Marshall, D. Lehnherr, B. D. Lindner, R. R. Tykwinski, *ChemPlusChem* **2017**, *82*, 967-1001.

[30] a) C. Reus, M. P. Lechner, M. Schulze, D. Lungerich, C. Diner, M. Gruber, J. M. Stryker, F. Hampel, N. Jux, R. R. Tykwinski, *Chem. Eur.J.* **2016**, *22*, 9097-9101; b) M. R. Rao, S. Johnson, D. F. Perepichka*, Org. Lett.* **2016**, *18*, 3574–3577; c) Z. Wang, J. Li, S. Zhang, Q. Wang, G. Dai, B. Liu, X. Zhu, Z. Li, C. Kolodziej, C. McCleese, C. Burda, W. Sun, L. Chen, *Chem. Eur. J.* **2018**, *24*, 14442-14447.

[31] Y. Gu, Y. G. Tullimilli, J. Feng, H. Phan, W. Zeng, J. Wu, *Chem. Commun.* **2019**, 55, 5567-5570.

[32] P. Demerseman, J. Einhorn, R. Royer, J.-F. O. Gourvest, *J. Heterocycl. Chem.* **1985**, *22*, 39-43.

[33] A. L. S. Thompson, G. W. Kabalka, M. R. Akula, J. W. Huffman, *Synthesis* **2005**, *2005*, 547-550.

[34] E. Weber, I. Csoregh, B. Stensland, M. Czugler, *J. Am. Chem. Soc.* **1984**, *106*, 3297–3306.

[35] T. Jousselin-Oba, K. Sbargoud, G. Vaccaro, F. Meinardi, A. Yassar, M. Frigoli, *Chem. Eur. J.,* **2017**, *23*, 16184-16188.

[36] A. Krasovskiy, F. Kopp, P. Knochel, *Angew. Chem. Int. Ed.* **2006**, *45*, 497-500; *Angew. Chem.* **2006**, *118*, 511-515.

[37] P. Bultinck, *Faraday Discuss.* **2007**, *135*, 347-365

[38] X. Shi, T. Y. Gopalakrishna, Q. Wang, C. Chi, *Chem. Eur. J.* **2017**, *23*, 8525-8531.

[39] a) A. Shimizu, Y. Tobe, *Angew. Chem., Int. Ed.* **2011**,*50*, 6906–6910; b) H. Miyoshi, S. Nobusue, A. Shimizu, I. Hisaki, M. Miyata, Y. Tobe, *Chem. Sci.* **2014**, *5*, 163-168.

[40] R. Herges, D. Geuenich, *J. Phys. Chem. A* **2001**, *105*, 3214-3220.

[41] R. Gershoni-Poranne, A. Stanger, *Chem. Eur. J.* **2014**, *20*, 5673-5688.

[42] CCDC depository number: 2107151.

[43] a) R. Englman, J. Jortner, *Mol. Phys.* **1970**, *18*, 145–164; b) J. V. Caspar, T. J. Meyer, *J. Phys. Chem.* **1983**, *87*, 952–957.

[44] Y.-C. Wei, S. F. Wang, Y. Hu, L.-S. Liao, D.-G. Chen, K.-H. Chang, C.-W. Wang, S.-H. Liu, W.-H. Chan, J.-L. Liao, W.-Y. Hung, T.-H. Wang, P.-T. Chen, H.-F. Hsu, Y. Chi, P.-T. Chou, *Nat. Photonics* **2020**, *14*, 570–577.

[45] Y. Cao, Y. Liang, L. Zhang, S. l. Osuna, A.-L. M. Hoyt, A. L. Briseno, K. N. Houk*, J. Am. Chem. Soc.* **2014**, *136*, 10743−1075.

[46] D. Doehnert, J. Koutecky, *J. Am. Chem. Soc.* **1980**, *102*, 1789-1796.

[47] a) T. Y. Gopalakrishna, W. Zeng, X. Lu, J. Wu, *Chem. Commun.* **2018**, 54, 2186. W. Zeng; b) J. Wu, Chem **2020**, *7*, 1–29.

[48] a) D. Chun, Y. Cheng, F. Wudl, *Angew. Chem. Int. Ed.* **2008**, *47*, 8380-8385; *Angew. Chem.* **2008**, *120*, 8508-8513; (b) E. Qu, C. Chi, C. *Org. Lett.* **2010**, *12*, 3360-3363.

[49] a) V. Coropceanu, J. Cornil, D. A. da Silva, Y. Olivier, R. Silbey and J.-L. Brédas, *Chem. Rev.* **2007**, *107*, 926–952; b) R. A. Marcus, *J. Chem. Phys.* **1956**, *24*, 966–978.

[50] J. Kang, N. Shin, D. Y. Jang, V. M. Prabhu, D. Y. Yoon, *J. Am. Chem. Soc.* **2008**, *130*, 12273–12275.

[51] H. Nakanotani, T. Higuchi, T. Furukawa, K. Masui, K. Morimoto, M. Numata, H. Tanaka, Y. Sagara, T. Yasuda, C. Adachi, *Nat. Commun.* **2014**, *5*, 4016

[52] a) S. Wang, X. Yan, Z. Cheng, H. Zhang, Y. Liu, Y. Wang, *Angew. Chem. Int. Ed.* **2015**, *54*, 13068–13072; *Angew. Chem.* **2015**, *127*, 13260-

13264; b) T. Yamanaka, H. Nakanotani, S. Hara, T. Hirohata, C. Adachi, *Appl. Phys. Exp.* **2017**, *10*, 074101.

[53] J. Brodeur, L. Hu, A. Malinge, E. Eizner, W. G. Skene, S. Kéna-Cohen, *Adv. Opt. Mater.* **2019**, *7*, 1901144.

[54] a) A. Zampetti, A. Minotto, F. Cacialli, *Adv. Funct. Mater.* **2019**, *29*, 1807623; b) Y. Yuan, Y. Hu, Y.-X. Zhang, J.-D. Lin, Y.-K. Wang, Z.-Q. Jiang, L.-S. Liao, S.-T. Lee, *Adv. Funct. Mater.* **2017**, *27*, 1700986,

[55] Y. Kage, S. Kang, S. Mori, M. Mamada, C. Adachi, D. Kim, H. Furuta, S. Shimizu, *Chem. Eur. J.* **2021**, *27*, 5259–5267.

[56] U. Balijapalli, R. Nagata, N. Yamada, H. Nakanotani, M. Tanaka, A. D'Aléo, V. Placide, M. Mamada, Y. Tsuchiya, C. Adachi, *Angew. Chem. Int. Ed.* **2021**, *60*, 8477–8482; *Angew. Chem.* **2021**, *133*, 8558-8563.

[57] J. Xue, Q. Liang, R. Wang, J. Hou, W. Li, Q. Peng, Z. Shuai, J. Qiao, *Adv. Mater.* **2019**, *31*, 1808242

[58] C. Li, R. Duan, B. Liang, G. Han, S. Wang, K. Ye, Y. Liu, Y. Yi, Y. Wang, *Angew. Chem. Int. Ed.* **2017**, *56*, 11525–11529; *Angew. Chem.* **2017**, *129*, 11683-11687.

Entry for the Table of Contents

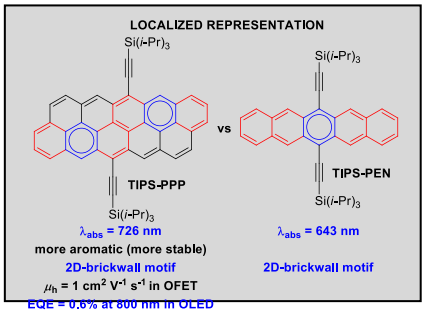

Acenes and *peri*-acenoacenes should be seen as π-conjugated systems containing one and two localized aromatic sextets, respectively, flanked with *ortho*-fused-diene fragments. The vertical extension of **TIPS-PEN**, namely **TIPS-PPP** has been prepared from a dione precursor and absorbs at longer wavelength, is 16 times more stable, exhibits 2D-brickwall motif in crystals with stronger π–π interactions and a lower reorganization energy. **TIPS-PPP** might be one of the best semiconductors in single-crystal-OFETs.